Two-dimensional hole gas in acceptor δ-doped GaAs

F. A. Reboredo and C. R. Proetto
Centro Atómico Bariloche and Instituto Balseiro, 8400 San Carlos de Bariloche, Rio Negro, Argentina
(Received 16 June 1992; revised manuscript received 9 October 1992)

Self-consistent calculations of the hole-subband structure of acceptor δ-doped GaAs are reported. Numerical results are obtained for the self-consistent potential, hole density, and subband energy levels. Many-body effects beyond the Hartree approximation, such as exchange and correlation, are included in the parabolic or diagonal approximation of the full Luttinger Hamiltonian within the density-functional formalism and are shown to be important . Results are also reported for the less ideal case of a doping profile with a Gaussian distribution of dopants.

I. INTRODUCTION

Doping semiconductors with donor or acceptor impurities have been traditionally an essential step in most of the basic research and industrial applications of these materials. In the last few years, and in pace with the continuous reduction of the spatial dimensions of semiconductor heterostructures and devices, the size of the dopant distribution has been decreased dramatically. One of the more promising doping techniques at the atomic level is clearly the δ doping, where the dopants are confined to one or a few atomic monolayers. This technique represents the ultimate control of a dopant profile and certainly will play an important role in future quantum-electronic and photonic-device research.

δ-doping profiles can be obtained by epitaxial growth methods such as molecular beam epitaxy (MBE): a distribution of atoms in a single monolayer is achieved by suspending the crystal growth and evaporating the dopant impurities on the nongrowing crystal surface. Subsequently regular crystal growth is resumed. Experiments have been carried out on n-type δ-doped GaAs layers or on δ-doped GaAs n-i-p-i heterostructures.[1,2] Only recently have single-acceptor (Be) doping spikes in GaAs also been investigated in detail.[3,4] Reference 3 essentially concentrates on the characterization of Be δ-doping layers in GaAs: a spatial localization of Be in δ-doped GaAs within a few lattice constants (< 20 Å) is reported from capacitance-voltage profiles and secondary ion mass spectroscopy. Reference 4, aimed to give a microscopic characterization of the two-dimensional hole gas (2DHG), reports photoluminescence studies, from where information about the subband hole structure was obtained. However, there were no theoretical results available for the valence subbands of p-type δ-doped GaAs. One of the motivations of the present work is just to fill this gap between experiment and theory.

On the theoretical side, while the self-consistent treatment of the two-dimensional electron gas (2DEG) at the n-type doping spikes is by now almost a standard calculation which gives a reasonable agreement with experiments,[5–7] much less is known about the properties of the equivalent 2DHG associated with p-type doping spikes. We are aware of only two previous self-consistent calculations on the properties of 2DHG: one by Broido and Sham,[8] where they studied the hole-subband structure for a GaAs p-channel inversion layer, and a second one by Ando,[9] related to the subband structure of 2DHG at GaAs/$Al_xGa_{1-x}As$ heterojunctions and quantum wells. One reason for the scarcity of theoretical studies on the 2DHG is that in order to give a rigorous description of the valence subbands one must deal with the full 4×4 matrix Luttinger Hamiltonian,[11] which is quite demanding from the computational viewpoint, as compared with the scalar problem posed by the 2DEG.

A second reason that complicates the study of 2DHG is that it is not yet clear to what extent the inclusion of many-body corrections is necessary in order to give a quantitative description of the subband structure; neither of the two previous calculations[8,9] includes many-body effects. We show here that the inclusion of many-body effects is important and leads to a better agreement with the experimental results of Ref. 4. We also provide a study of the subband-hole structure for the more general case of a doping profile with a Gaussian distribution, instead of a sharp δ-function doping profile.

The rest of the paper is organized as follows: in Sec. II we define our model and give all the necessary formulas; Sec. III is dedicated to a comparison among the numerical results for the self-consistent potentials, hole densities, and subband energies corresponding to different approximations; in Sec. IV we present the results for the Gaussian doping profile, and finally in Sec. V we give the conclusions.

II. MODEL AND METHOD OF CALCULATION

For the general treatment of the valence bands, one should use the 6×6 Luttinger-Kohn $\mathbf{k} \cdot \mathbf{p}$ Hamiltonian.[10] However, the spin-orbit splitting Δ between the $J = 3/2$ and the $J = 1/2$ multiplet is about 340 meV for GaAs so

the spin-splitoff band can be ignored, and consequently the original 6×6 $\mathbf{k} \cdot \mathbf{p}$ Hamiltonian reduces to the 4×4 Luttinger Hamiltonian.[11]

We assume that the negative charge of the ionized acceptor impurities is homogeneously smeared out in the plane perpendicular to the growth direction (jellium approximation), neglecting the point-charge character of the dopants and the spatial potential fluctuations which result from the random distributions of impurities in the doped planes. We restrict ourselves in the present calculations to a rather high dopant concentration ($\sim 10^{13}/\mathrm{cm}^2$) so as to fulfill this approximation in a reasonable degree.

We consider a periodic sequence of p-type δ-doped planes, immersed in an otherwise homogeneous GaAs host matrix, grown in a [100] direction, which we take along the quantization axis z. Due to translational symmetry in the (x, y) plane of our system, the wave functions can be written as a plane wave along this plane times a wave function along z, given by the solution of the following 4×4 effective mass matrix Hamiltonian:

$$\sum_{j=1}^{4}[H^0_{i,j}(k_x, k_y, \hat{k}_z) + V(z)\delta_{i,j}]\psi_{jn\mathbf{k}}(z) = E_n(\mathbf{k})\psi_{in\mathbf{k}}(z) \quad (i = 1, 2, 3, 4), \quad (1)$$

where $V(z)$ is the periodic potential, $\psi_{in\mathbf{k}}(z)$ the four-component envelope wave function corresponding to subband index n and wave vector $\mathbf{k}$ with eigenvalue $E_n(\mathbf{k})$, and $\hat{k}_z$ is the operator $-i\partial/\partial z$.

The 4×4 Luttinger matrix (the kinetic energy) is given by

$$H^0 = \begin{Bmatrix} P+Q & R & -S & 0 \\ R^* & P-Q & 0 & S \\ -S^* & 0 & P-Q & R \\ 0 & S^* & R^* & P+Q \end{Bmatrix}, \quad (2)$$

where

$$P \pm Q = \frac{\hbar^2}{2m}[(\gamma_1 \mp 2\gamma_2)\hat{k}_z^2 + (\gamma_1 \pm \gamma_2)k_\parallel^2], \quad (3)$$

$$R = \sqrt{3}\frac{\hbar^2}{2m}[\gamma_2(k_x^2 - k_y^2) - 2i\gamma_3 k_x k_y], \quad (4)$$

$$S = \sqrt{3}\frac{\hbar^2}{m}\gamma_3(k_x - ik_y)\hat{k}_z \quad (5)$$

with m the free electron mass, $k_\parallel^2 = k_x^2 + k_y^2$ and γ_1, γ_2, and γ_3 the Luttinger parameters appropriate for GaAs. In writing H^0 we have neglected very small linear k terms caused by the lack of inversion symmetry of the GaAs zinc-blende structure.[8]

The 4×4 matrix (2) can be block diagonalized by a change of basis into two independent matrices H^U and H^L

$$\tilde{H}^0 = \begin{Bmatrix} H^U & 0 \\ 0 & H^L \end{Bmatrix} \quad (6)$$

with the explicit expressions

$$H^\sigma = \begin{bmatrix} P \pm Q & \tilde{R} \\ \tilde{R}^* & P \mp Q \end{bmatrix}, \qquad \tilde{R} = |R| - i\hat{k}_z|S|, \quad (7)$$

where $\sigma = U$ (L) refers to the upper (lower) $\pm$ signs. The unitary matrix that block diagonalizes H^0 depends on k_x and k_y but is independent of $\hat{k}_z$; the explicit expression of the matrix can be found in Ref. 8. The upper- and lower-block envelope functions satisfy

$$\sum_{j=1}^{2}[H^\sigma_{i,j}(k_x, k_y, \hat{k}_z) + V(z)\delta_{i,j}]\psi^\sigma_{jn\mathbf{k}}(z) = E^\sigma_n(\mathbf{k})\psi^\sigma_{in\mathbf{k}}(z) \quad (i = 1, 2), \quad (8)$$

where $\psi^\sigma_{in\mathbf{k}}(z)$ are now two-component envelope wave functions.

The still undefined potential $V(z)$ is the superlattice potential, which is given by the sum of the potential of the ionized impurities $V_I(z)$ and the Hartree potential $V_H(z)$

$$V(z) = V_I(z) + V_H(z) \quad (9)$$

and is determined self-consistently from the Schrödinger equation (8) and Poisson equation:

$$\frac{d^2}{dz^2}V(z) = -\frac{4\pi e^2}{\epsilon}\rho(z), \quad (10)$$

where ϵ is the static dielectric constant of GaAs and $\rho(z)$ is given by

$$\rho(z) = -N_a \sum_{j=-\infty}^{\infty} \delta(z - jd) + n(z) \quad (11)$$

with N_a the two-dimensional concentration of ionized acceptor impurities, d the superlattice period, and $n(z)$ the hole density at point z. One has for the model used here

$$n(z) = \sum_{\sigma i n\mathbf{k}} |\psi^\sigma_{in\mathbf{k}}(z)|^2 f[E_F - E^\sigma_n(\mathbf{k})], \quad (12)$$

where E_F is the Fermi level and $f(x)$ the Fermi-Dirac function. We adopt the following boundary conditions for the Poisson equation:

$$V_I(d/2) + V_H(d/2) = 0 \quad (13)$$

and

$$V(z) = V(z + d), \quad (14)$$

where (13) is equivalent to adopting the value of the self-consistent potential at the midpoint between two consecutive acceptor planes as the origin of energies.

The constraint of electrical neutrality is expressed by the condition that the integral over one period of $\rho(z)$ should be zero so (11) can be rewritten as

$$N_a = \frac{1}{\Omega}\sum_{\sigma n\mathbf{k}} f[E_F - E^\sigma_n(\mathbf{k})] \quad (15)$$

with Ω the sample area.To calculate the two-dimensional sums on k_x and k_y in Eqs. (12) and (15), we have defined a grid in the reciprocal space. Using the symmetries of (8), the summation can be restricted to one-eighth of the full space, and typically the grid size was about 325 points. While an analytical solution of (8) is not possible, the structure of H^U and H^L suggests the following numerical strategy. We first observe upon neglecting the off-diagonal terms that (8) is split into two (each doubly degenerate) single-component equations:

$$\left[-\frac{\hbar^2}{2m}(\gamma_1 \mp 2\gamma_2)\frac{d^2}{dz^2} + V(z)\right]\Phi^{h}_{n,k_z}{}^{\ell}(z) = E^{h}_{n}{}^{\ell}(k_z)\Phi^{h}_{n,k_z}{}^{\ell}(z), \quad (16)$$

where

$$E^{h}_{n}{}^{\ell}(k_z) = E^{h}_{n}{}^{\ell}(\mathbf{k}) - \frac{\hbar^2}{2m}(\gamma_1 \pm \gamma_2)k_{\|}^2. \quad (17)$$

We will refer to Eq. (16) as the parabolic approximation, as all the nonparabolicities embodied in the complete equation (8) are lost in this approximation. An attractive feature of Eq. (16) is that as a consequence of the neglect of the nondiagonal terms, the mixing between heavy and light holes is zero, and the 2DHG splits into two perfectly defined components, one heavy, with perpendicular (parallel) mass $m_{\perp}^{\mathrm{hh}} = m/(\gamma_1 - 2\gamma_2)$ $[m_{\|}^{\mathrm{hh}} = m/(\gamma_1 + \gamma_2)]$, and a light component, with perpendicular (parallel) mass $m_{\perp}^{\mathrm{lh}} = m/(\gamma_1 + 2\gamma_2)$ $[m_{\|}^{\mathrm{lh}} = m/(\gamma_1 - \gamma_2)]$. For later use, we give the explicit parabolic version of Eq. (15) at zero temperature, which by performing analytically the sums on $k_{\|}$ becomes

$$N_a = \frac{m_{\|}^{\mathrm{hh}}}{\pi\hbar^2}\sum_{n,k_z}[E_F - E_n^h(k_z)]\Theta[E_F - E_n^h(k_z)] + \frac{m_{\|}^{\mathrm{lh}}}{\pi\hbar^2}\sum_{n,k_z}[E_F - E_n^{\ell}(k_z)]\Theta[E_F - E_n^{\ell}(k_z)] \quad (18)$$

with $\Theta[x]$ the Heaviside step function.

The self-consistent solutions of (16) are obtained by performing a plane wave expansion of the periodic part of $\Phi^{h}_{n,k_z}{}^{\ell}(z)$, which essentially transforms (16) into a typical matrix eigenvalue problem. More details on this particular step of the calculation can be found in Ref. 7.

The self-consistent solution of (16) yields an infinite set of doubly degenerate heavy- and light-hole subband energies and wave functions, and we use this basis to expand the solutions $\psi^{\sigma}_{in\mathbf{k}}(z)$ of the exact eigenvalue equation (8), as follows:

$$\psi^{\sigma}_{1n\mathbf{k}}(z) = \sum_{m=1}^{\infty}[A^{\sigma}_{1nm}(\mathbf{k})\Phi^{h}_{m,k_z}(z) + B^{\sigma}_{1nm}(\mathbf{k})\Phi^{\ell}_{m,k_z}(z)], \quad (19)$$

$$\psi^{\sigma}_{2n\mathbf{k}}(z) = \sum_{m=1}^{\infty}[A^{\sigma}_{2nm}(\mathbf{k})\Phi^{h}_{m,k_z}(z) + B^{\sigma}_{2nm}(\mathbf{k})\Phi^{\ell}_{m,k_z}(z)]. \quad (20)$$

If the summations in Eqs. (19) and (20) run over all the self-consistent solutions of the parabolic equation (16), $\psi^{\sigma}_{1n\mathbf{k}}(z)$ and $\psi^{\sigma}_{2n\mathbf{k}}(z)$ are the exact solutions of (8). In practice , M heavy-hole states and N light-hole states are retained and (8) is diagonalized inside this $(M+N)$-dimensional subspace. We take $M = N = 10$ in Eqs. (19) and (20), which gives an accurate description of the subbands up to the Fermi energy for the range of parameters investigated.

While our method of solution is similar in spirit to the already mentioned calculations on the properties of 2DHG in p-type inversion layers and GaAs/Al_xGa_{1-x}As heterostructures and quantum wells, we differ in some points: (i) In Ref. 8 the band warping is neglected by replacing γ_2 and γ_3 by their arithmetic average. In this axial approximation the Hamiltonian (1) depends only on $k_{\|}$ and the calculation simplifies considerably, as, for example, the two-dimensional summation in Eq. (12) reduces to a one-dimensional summation on $k_{\|}$. Furthermore a variational $k_{\|} = 0$ non-self-consistent solution of (16) was generated as a basis for the expansions in (19) and (20), and only two heavy and two light solutions of (16) were used in the expansion, which in the light of the results of Ref. 9 and the present calculation is insufficient in order to get reliable quantitative results. (ii) In Ref. 9 two different methods were used: an intermediate self-consistent basis was employed in order to solve a GaAs/Al_xGa_{1-x}As heterojunction while a Fourier expansion of the periodic part of the two-component $\psi^{\sigma}_{in\mathbf{k}}(z)$ was attempted to solve a multiple quantum-well problem. Our method of solution is essentially a combination of both: an intermediate parabolic anisotropic self-consistent basis is generated by performing a Fourier[7] expansion and subsequently the full Hamiltonian is projected on this intermediate basis. While more involved from the programming viewpoint, it is by far more efficient in the numerical sense: as the parabolic basis is close to the solution of the full equation (8), this allows us to obtain excellent convergence with a relatively small intermediate basis.

While the method of calculation presented in this section is valid for any value of the period d, by increasing this period one can move from the superlattice regime to the multiple quantum well or atomic regime, where each quantum well is effectively disconnected from its neighboring wells. As the experimental works mentioned in the Introduction were performed for a single layer or quantum well, we restrict the present calculation to the atomic limit by taking $d = 1000$ Å and including only the states at $k_z = 0$, where k_z is the Bloch index in the z direction.

III. SELF-CONSISTENT POTENTIALS, HOLE DENSITIES, AND SUBBAND ENERGY LEVELS

All the numerical results that follow correspond to the zero-temperature limit $T = 0$ and $N_a = 8 \times 10^{12}/\mathrm{cm}^2$ (taken from Ref. 4); also $\gamma_1 = 6.85$, $\gamma_2 = 2.1$, $\gamma_3 = 2.9$, and $\epsilon = 12.5$, as corresponds to bulk GaAs.

As a first rough approximation to the present prob-

lem, one can solve Eq. (16) by neglecting any screening effect [$V_H(z) \equiv 0$ in Eq. (9)], in which case the potential $V(z)$ is just the bare V-shaped potential associated with an uniformly charged plane, whose exact analytical solution[12,13] gives two occupied subbands, one heavy and one light, with an energy splitting of about 43 meV. With these subband energies, from (18) it is easy to obtain a Fermi level that lies 90 meV above the ground heavy-hole subband.

When screening (in the Hartree approximation) is included in the calculation, the self-consistent solution of Eq. (16) gives the potential and level structure displayed in Fig. 1: the softening of the nonscreened V-shaped potential yields now six occupied subbands (4 heavy, 2 light), an energy splitting of about 21.5 meV between the first heavy- and light-hole subbands, and the Fermi level lies 66 meV above the ground-state heavy-hole subband. Using again Eq. (18), but replacing this time the level structure of Fig. 1, it is simple to obtain that most of the holes are distributed almost equally between the two lowest subbands. This is due to the fact that what really matters for the calculation of the subband density in (18) is the energy difference between the Fermi level and the subband energy times the effective parallel mass; as $E_F - E_1^h > E_F - E_1^\ell$, while $m_{\|}^{\rm hh} < m_{\|}^{\rm lh}$, there is a compensation between these two factors and each of the two lowest subbands accommodates approximately half of the total density.

Finally, the self-consistent solution of Eq. (8), which includes screening and nonparabolicities, gives the results presented in Fig. 2: two occupied subbands, an energy splitting of about 20 meV between the two occupied subbands, and about 34 meV from the ground-state subband to the Fermi level.

From the comparison between Figs. 1 and 2 it is clear that while the self-consistent potential and subband energy levels are not quite sensitive to the nonparabolicities, the Fermi level decreases dramatically (32 meV) when the full Luttinger Hamiltonian is included in the calculation. This is related to the increase of the ground state in-plane effective mass over its value $m/(\gamma_1 + \gamma_2)$ of the parabolic approximation: being the ground state of the system, the only possible contribution of the off-diagonal elements is to lower its energy, thereby increasing its in-plane mass. This in turn implies that the ground-state subband is able to accommodate more carriers, lowering the Fermi level. For the set of parameters corresponding to Fig. 2, about 82% (18%) of the carriers are in the ground-state (first excited-state) subband. The hole density distributions associated with the potentials and energy levels of Figs. 1 and 2 are displayed in Fig. 3: the pointed line corresponds to the parabolic self-consistent solutions, while the dashed line corresponds to the Luttinger self-consistent solution. As can be seen, the already discussed large lowering of the Fermi level has been achieved by very small changes in the total hole density, in spite of the fact that the ground-state subband has a much greater occupancy in the Luttinger

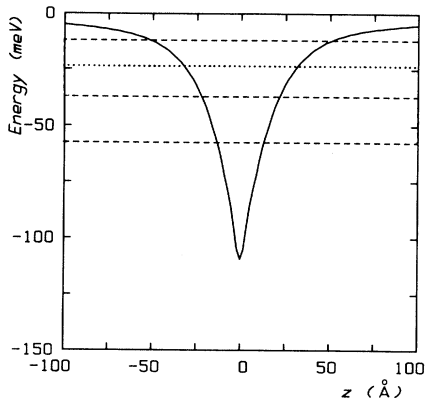

FIG. 2. Luttinger self-consistent potential (solid line), subband level structure at $k_{\|} = 0$ (dashed lines), and Fermi level (dotted line) in the Hartree approximation.

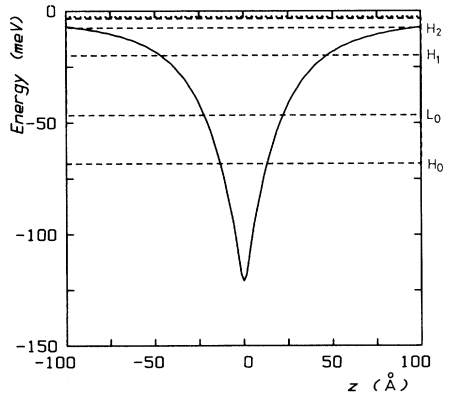

FIG. 1. Parabolic self-consistent potential (solid line), subband structure at $k_{\|} = 0$ (dashed lines), and Fermi level (dotted line) in the Hartree approximation. While there are in principle six subbands below the Fermi level, essentially all the charge is concentrated in the two lowest heavy-hole (H_0) and light-hole (L_0) subbands.

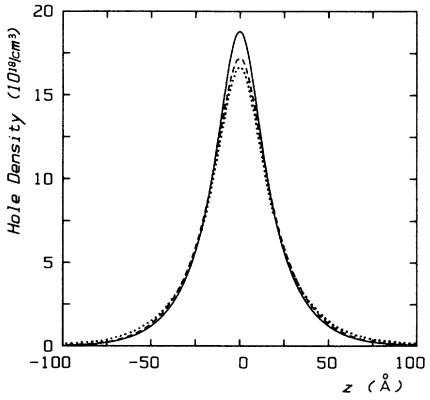

FIG. 3. Total hole densities: dotted line, parabolic self-consistent (Hartree) approximation; dashed line, Luttinger self-consistent (Hartree) approximation; solid line, parabolic self-consistent (Hartree and exchange-correlation) approximation.

self-consistent approximation than in the parabolic one. This can be understood when we realize that as soon as $k_{\|} \neq 0$, the off-diagonal elements of the Luttinger Hamiltonian produce a strong mixing between the heavy- and light-hole states of the parabolic approximation, but in such a way that when the Luttinger self-consistent density is projected back to the parabolic self-consistent basis we find the remarkable result that the holes are concentrated again almost equally between the two lowest parabolic subbands. Since the charge densities are quite similar it is not surprising to find the similarity between the self-consistent potentials and subband energy levels displayed in Figs. 1 and 2. However, the confrontation of the previous theoretical results with the experimental data of Ref. 4 reveals a considerable discrepancy: from the energy difference between the emission peaks of the photoluminiscence spectra an energy splitting of 36 meV between the two lowest subbands is reported, and at low intensity illumination, the Fermi level lies about 50 meV above the first peak. These experimental results should be compared with the 21.5 meV (20 meV) and 66 meV (34 meV) theoretical results of the parabolic (Luttinger) self-consistent approximation, respectively.

This discrepancy leads us to an essentially unexplored area of semiconductor heterostructures: the importance of many-body corrections beyond the Hartree approximation for the 2DHG. An attractive way to study the exchange-correlation effect on the subband structure of heterostructures and quantum wells is to use the density-functional method.[14–16] In this formulation, the effect is taken into account by introducing an exchange-correlation potential $V_{\rm XC}[n(z)]$ which is given by a functional derivative of the exchange correlation part of the ground-state energy with respect to the particle density. In the simplest approximation (the local density approximation or LDA) the exchange-correlation potential energy is approximated by the exchange correlation contribution to the chemical potential of a homogeneous gas having a uniform density which is equal to the local density $n(z)$ of the inhomogeneous system.

However, there are some problems in the choice of $V_{\rm XC}$ in our system. While for the parabolic and isotropic gas of spin-$\frac{1}{2}$ particles there are in the literature several simple and quite accurate parametrizations of the $V_{\rm XC}$ within the LDA, we are not aware of any equivalent parametrization for the four-component, anisotropic and nonparabolic hole gas. Faced with this difficulty, and encouraged by the almost identical results for the charge density and subband energy levels for the parabolic self-consistent and Luttinger self-consistent calculations, we have included the many-body corrections in the parabolic approximation. By analogy with the spin-density functional formalism,[17] the exchange-correlation potential is different for the heavy- and light-hole gases and consequently the inclusion of many-body effects in the parabolic approximation within the LDA amounts to redefining the self-consistent potential

$$V^{\alpha}(z) = V_I(z) + V_H(z) + V_{\rm XC}^{\alpha}[n^h(z), n^{\ell}(z)], \qquad (21)$$

where α refers to heavy or light holes. Neglecting the correlation between heavy and light holes $V_{\rm XC}^{h}$ ($V_{\rm XC}^{\ell}$) depends only on the hole density in the heavy (light) subbands.

Among the many possibilities for $V_{\rm XC}(z)$ available in the literature, we have chosen the parametrized expression of Perdew and Zunger[18] that seems to give accurate results over a wide range of densities; for the effective masses in $V_{\rm XC}$ we have used the isotropic heavy-hole mass $m^h = 0.62m$ and light-hole mass $m^{\ell} = 0.072m$ as calculated in Ref. 19. Combescot and Nozières[20] have calculated the effect of the anisotropy on the exchange-correlation contribution to the total energy and found the effect to be quite small. The corresponding self-consistent potential and energy levels are displayed in Fig. 4: besides a common deepening of the self-consistent potential, the greater density of the heavy-hole gas gives rise to a splitting between the two self-consistent potentials of about 6 meV. The inclusion of many-body effects decreases the number of occupied subbands from six (Fig. 1) to three (2 heavy, 1 light), but what is more important, it increases the energy splitting between the ground-state heavy- and light-hole subbands to about 26 meV, in better agreement with the experimental values. The solid line of Fig. 3 shows the corresponding hole density distribution: the inclusion of many-body effects decreases the Coulomb repulsion between holes with the same spin, and the holes concentrate closer to the impurity charged plane.

While the use of the parabolic approximation allows us to include exchange-correlation effects in the calculation, an intrinsic failure of this approximation, already discussed, is that it gives a not quite reliable Fermi level position, as a consequence of the neglect of nonparabolicities. By analogy with the difference in Fermi level positions between Figs. 1 and 2, we believe that a more rigorous treatment of many-body corrections, including explicitly the nonparabolicities, should give a Fermi level which lies between the second and third occupied subbands of Fig. 4.

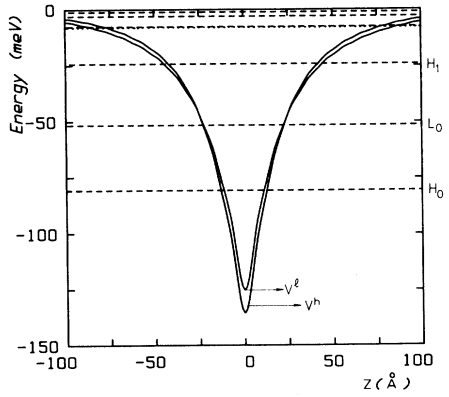

FIG. 4. Parabolic heavy-hole $[V^h(z)]$ and light-hole $[V^{\ell}(z)]$ potentials (solid lines) including many-body corrections. The dashed lines give the subband level structure at $k_{\|} = 0$ and the dotted line the Fermi level position.

IV. GAUSSIAN DOPING PROFILE

With the purpose of investigating the dependence of the results of the previous section on the assumption of a perfectly sharp-defined doped plane, we have given a finite width to the doping profile.

Figure 5 shows the corresponding results obtained in the parabolic self-consistent approximation (including many-body corrections) for the $k_{\|} = 0$ subband level structure, Fermi level, and bottom of the heavy- and light-hole potentials as a function of the Gaussian width (σ) of the dopant profile. Due to our choice of origin of energies as the value of the self-consistent potential at $z = d/2$, which is different for each value of σ, only differences of energy should be compared in Fig. 5 and not absolute values.

As expected, the increasing of the doping profile leads to a decrease of the subband spacing, as the self-consistent potential becomes shallow. As a consequence of this flattening of the potential the number of occupied subbands increases from three ($\sigma = 0$) to six ($\sigma = 100$ Å). It should be remarked, however, that while we expect to have a rather accurate description of the self-consistent potential subband level, the Fermi level position is not reliable and should be much lower with nonparabolicities included in the calculation.

The many-body corrections, as measured by the energy difference between the bottom heavy- and light-hole potentials, are also less important as σ grows; that is due to the fact that as the potential becomes increasingly shallow, the heavy- and light-hole densities decrease by extending further away, and the corresponding corrections follow the same trend. It is interesting to note that the effect is particularly noticeable for $\sigma \lesssim 30$–40 Å.

V. CONCLUSIONS

We have studied the hole subband structure of acceptor δ-doped GaAs. As a first approach to the problem, we calculated the self-consistent potential, hole density, and subband energy levels of the full Luttinger Hamiltonian, including screening in the Hartree approximation. Considerable discrepancies between these theoretical results with experiments led us to investigate the effect of many-body corrections beyond the Hartree approximation, such as exchange and correlation. Guided by the strong similarity between the self-consistent solutions of the full Luttinger Hamiltonian and its parabolic approximation, we included the exchange and correlation effects in the latter approximation, using the formalism of the density-functional method.

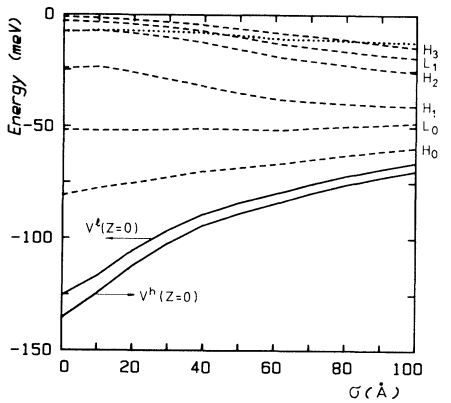

FIG. 5. Energy levels (dashed lines) and Fermi level (pointed line) as a function of the width of the Gaussian doping profile. The two solid lines correspond to the bottom of the heavy-hole and light-hole potentials.

The density of the heavy-hole subband being greater than the density of the light-hole subband near the doped plane, the many-body corrections (which in the LDA only depend on the density) lead to a sizable renormalization of the self-consistent heavy-hole and light-hole potentials, which in turn gives rise to an additional splitting of the first heavy- and light-hole subbands, driving the theoretical splitting into better (but not perfect) agreement with the experimental splitting. More theoretical and experimental work is clearly necessary to clarify this remaining discrepancy.

We also investigated the modifications introduced in the previous results when we relax the condition of perfect δ doping, by giving a finite width to the distribution of doping impurities. As expected, increasing the doping profile leads to a shallow self-consistent potential, and a decrease of the subband spacing and of the importance of exchange-correlation effects.

ACKNOWLEDGMENTS

F.A.R. would like to thank the Consejo Nacional de Investigaciones Cientifícas y Técnicas (CONICET) of Argentina for financial support.

[1] F. Koch and A. Zrenner, Mater. Sci. Eng. B **1**, 221 (1989).
[2] E. F. Schubert, Opt. Quantum Electron. **22**, 5141 (1990).
[3] E. F. Schubert, J. M. Kuo, R. F. Kopf, H. S. Luftman, L. C. Hopkings, and N. J. Sauer, J. Appl. Phys. **67**, 1969 (1990).
[4] J. Wagner, A. Ruiz, and K. Ploog, Phys. Rev. B **43**, 12 134 (1991).
[5] A. Zrenner, F. Koch, and K. Ploog, Surf. Sci. **196**, 671 (1988).
[6] M. H. Degani, Phys. Rev. B **44**, 5580 (1991).
[7] F. A. Reboredo and C. R. Proetto, Solid State Commun. **81**, 163 (1991).
[8] D. A. Broido and L. J. Sham, Phys. Rev. B **31**, 888 (1985).
[9] T. Ando, J. Phys. Soc. Jpn. **54**, 1528 (1985).
[10] J. M. Luttinger and W. Kohn, Phys. Rev. **97**, 869 (1955).
[11] J. M. Luttinger, Phys. Rev. **102**, 1030 (1956).
[12] E. F. Schubert, T. D. Harris, J. E. Cunningham, and W. Jan, Phys. Rev. B **39**, 11 011 (1989).
[13] J. M. Ferreyra and C. R. Proetto, Phys. Rev. B **42**, 5657 (1990).
[14] P. Hohenberg and W. Kohn, Phys. Rev. **136**, B864 (1964).

[15]W. Kohn and L. J. Sham, Phys. Rev. **140**, A1133 (1965).
[16]L. J. Sham and W. Kohn, Phys. Rev. **145**, 561 (1966).
[17]W. Kohn and P. Vashishta, in *Theory of the Inhomogeneous Electron Gas*, edited by S. Lundqvist and N. H. March (Plenum, New York, 1983), p. 79.
[18]J. Perdew and A. Zunger, Phys. Rev. B **23**, 5048 (1981).
[19]W. F. Brinkman and T. M. Rice, Phys. Rev. B **7**, 1508 (1973).
[20]M. Combescot and P. Nozières, J. Phys. C **5**, 2369 (1972).